# BMP9 and BMP10 are necessary for proper closure of the ductus arteriosus

Sandrine Levet[a,b,c,1], Marie Ouarné[a,b,c,1], Delphine Ciais[a,b,c], Charles Coutton[c,d,e], Mariela Subileau[a,b,c], Christine Mallet[a,b,c], Nicolas Ricard[a,b,c], Marie Bidart[a,b,c], Thierry Debillon[f], Francesca Faravelli[g], Caroline Rooryck[h], Jean-Jacques Feige[a,b,c], Emmanuelle Tillet[a,b,c,2], and Sabine Bailly[a,b,c,2,3]

[a]Institut National de la santé et de la Recherche Médicale (INSERM, U1036), Grenoble, France F-38000; [b]Commissariat à l'Énergie Atomique et aux Energies Alternatives, Institut de Recherches en Technologies et Sciences pour le Vivant, Laboratoire Biologie du Cancer et de l'Infection, Grenoble, France F-38000; [c]Université Grenoble-Alpes, Grenoble, France F-38000; [d]Laboratoire de Génétique Chromosomique, Département de Génétique et Procréation, Hôpital Couple Enfant, Centre Hospitalier Universitaire de Grenoble, Grenoble F-38000, France; [e]Equipe "Génétique, Infertilité et Thérapeutique," Laboratoire Andrologie Gérontechnologie Inflammation Modélisation, CNRS FRE3405, Grenoble, France F-38000; [f]Service de Médecine et Réanimation Néonatale, Centre Hospitalier Universitaire de Grenoble, Grenoble, France F-38000; [g]Division of Medical Genetics, Galliera Hospital, Genoa, Italy; and [h]Service de Génétique Médicale, Centre Hospitalier Universitaire de Bordeaux, Bordeaux, France F-33000

Edited by Napoleone Ferrara, University of California, San Diego, La Jolla, CA, and approved May 19, 2015 (received for review April 30, 2015)

**The transition to pulmonary respiration after birth requires rapid alterations in the structure of the mammalian cardiovascular system. One dramatic change that occurs is the closure of the ductus arteriosus (DA), an arterial connection in the fetus that directs blood flow away from the pulmonary circulation. Two members of the TGFβ family, bone morphogenetic protein 9 (BMP9) and BMP10, have been recently involved in postnatal angiogenesis, both being necessary for remodeling of newly formed microvascular beds. The aim of the present work was to study whether BMP9 and BMP10 could be involved in closure of the DA. We found that *Bmp9* knockout in mice led to an imperfect closure of the DA. Further, addition of a neutralizing anti-BMP10 antibody at postnatal day 1 (P1) and P3 in these pups exacerbated the remodeling defect and led to a reopening of the DA at P4. Transmission electron microscopy images and immunofluorescence stainings suggested that this effect could be due to a defect in intimal cell differentiation from endothelial to mesenchymal cells, associated with a lack of extracellular matrix deposition within the center of the DA. This result was supported by the identification of the regulation by BMP9 and BMP10 of several genes known to be involved in this process. The involvement of these BMPs was further supported by human genomic data because we could define a critical region in chromosome 2 encoding eight genes including *BMP10* that correlated with the presence of a patent DA. Together, these data establish roles for BMP9 and BMP10 in DA closure.**

ductus arteriosus | BMP9 | BMP10 | endMT | pediatric

The ductus arteriosus (DA) is a large blood vessel whose obstruction is essential for the transition from fetal to neonatal circulation. It is a fetal arterial shunt connecting the pulmonary artery with the aortic arch. During fetal life, the DA directs deoxygenated blood away from the pulmonary circulation and toward the descending aorta, bypassing the nonventilated fetal lungs. After birth, the DA closes spontaneously within 1–3 h in small rodents or within 24–48 h in human newborns (1, 2). Although an open DA is required for fetal survival, the persistence of a patent DA (PDA) after birth is a major cause of morbidity and mortality, particularly in preterm neonates, leading to severe complications, including pulmonary hypertension, right ventricular dysfunction, postnatal infections, and respiratory failure. The incidence of PDA has been estimated to be one in 500 in-term newborns and accounts for the majority of all cases of congenital heart disease in preterm newborns. It is currently believed that DA closure involves a two-step process (3, 4). The first, provisional closure, also called functional closure, occurs at birth and is accomplished by smooth muscle cell contraction and DA constriction. The second step, named anatomical closure, involves a profound remodeling of cells within the former DA lumen and permits permanent closure of the DA. Although several factors have been implicated in DA closure (oxygen tension, prostaglandin E2, laminin, growth hormone, and platelets), the precise molecular and cellular signals that promote the transition from initial constriction to definitive DA closure are not yet fully understood.

Bone morphogenetic protein 9 (BMP9) and BMP10 are two members of the BMP family that have been demonstrated to play major roles in vascular development (5). In 2007, it was demonstrated that BMP9 and BMP10 bind with high affinity to the endothelial-specific receptor activin receptor-like kinase 1 (ALK1), a type 1 receptor of the TGFβ family (6) whose mutations are involved in vascular diseases (5). Both BMP9 and BMP10 are present in blood, and their circulating levels are particularly elevated in mice around birth (7, 8), suggesting that they could play a role in pre- and postnatal development. In the present work, we addressed whether BMP9 and BMP10 could be involved in DA closure. For this purpose, we used *Bmp9*-KO mice and neutralizing anti-BMP10 antibody. Herein, we show that injection of a neutralizing anti-BMP10 antibody into *Bmp9*-KO pups led to an open DA and identified several targets that may be involved in this closure defect. This work is further supported by human genomic data, based on the definition of a 700-kb minimal critical region in chromosome 2 encoding eight genes, including *BMP10*, that correlated with the presence of a

## Significance

**At birth, newborns must switch from the fetal aquatic life to the aerial one, by closure of a vessel named the ductus arteriosus. During fetal life, it allows blood to bypass the lungs, and a failure of its closure at birth is a major cause of mortality, particularly in preterm neonates. This pathological condition is known as patent ductus arteriosus and occurs in approximately 60% of preterm infants born before 28 wk of gestation. Herein, we show, for the first time to our knowledge, the involvement of two circulating growth factors, bone morphogenetic proteins BMP9 and BMP10, in the anatomical closure of this vessel. This finding will have potential clinical applications in the management of this pathology.**

Author contributions: S.L., M.O., D.C., J.-J.F., E.T., and S.B. designed research; S.L., M.O., D.C., M.S., C.M., N.R., M.B., E.T., and S.B. performed research; C.C., F.F., and C.R. contributed new reagents/analytic tools; S.L., M.O., D.C., C.C., T.D., E.T., and S.B. analyzed data; and S.L., M.O., J.-J.F., E.T., and S.B. wrote the paper.

The authors declare no conflict of interest.

This article is a PNAS Direct Submission.

[1]S.L. and M.O. contributed equally to this work.

[2]E.T. and S.B. contributed equally to this work.

[3]To whom correspondence should be addressed. Email: sabine.bailly@cea.fr.

This article contains supporting information online at www.pnas.org/lookup/suppl/doi:10.1073/pnas.1508386112/-/DCSupplemental.

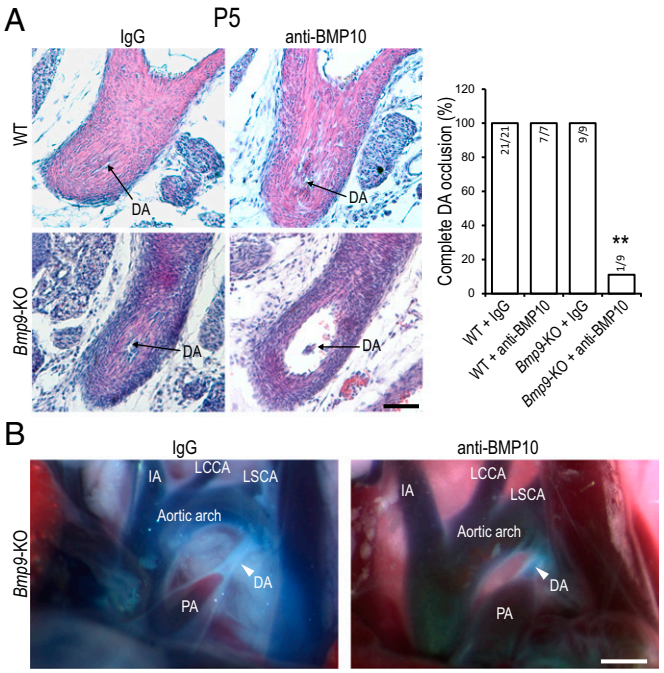


**Fig. 1.** *Bmp9*-KO pups treated with an anti-BMP10 antibody have an open ductus arteriosus (DA) at P5. *Bmp9*-KO pups were treated at P1 and P3 with IgG or an anti-BMP10 antibody and killed at P5. (*A*) Representative hematoxylin and eosin (H&E) staining of transverse sections of DA. WT pups treated with IgG ($n = 21$) from 10 littermates or with anti-BMP10 ($n = 7$) from 3 littermates; *Bmp9*-KO pups treated with IgG ($n = 9$) from 7 littermates or with anti-BMP10 ($n = 9$) from 6 littermates. (Scale bars: 50 μm.) The graph bar indicates the number of mice with complete DA occlusion over the total number of mice investigated. The Fisher's exact test was used to compare the different groups (**$P \leq 0.01$). (*B*) Representative angiographic images after Evans blue injection of the great arteries and the DA. B*mp9*-KO pups treated with IgG ($n = 3$) or with anti-BMP10 ($n = 5$) from 3 littermates. IA, innominate artery; LCCA, left common carotid artery; LSCA, left subclavian artery; PA, pulmonary artery. (Scale bars: 500 μm.)

PDA in two patients. This work thus identifies a previously unidentified signaling pathway, the BMP9/10 pathway, in the anatomical closure of the DA.

## Results

**Injection of Antibodies Directed Against BMP10 in *Bmp9*-KO Pups Leads to an Open DA at P5.** To address the role of BMP9 and BMP10 in postnatal vascular remodeling, we used *Bmp9*-KO pups, which are fine and viable. They were injected at postnatal day 1 (P1) and P3 with a neutralizing anti-BMP10 antibody as previously described (8) because we could not use *Bmp10*-KO pups, which die at midgestation due to cardiac defects (9). We first analyzed transverse sections of the DA at P5 after hematoxylin and eosin (H&E) staining. We found that *Bmp9*-KO pups treated with an anti-BMP10 antibody had an open DA whereas the other pups (WT pups injected or not with an anti-BMP10 antibody or *Bmp9*-KO pups) had a closed DA at P5 (Fig. 1*A*); only 1 out of 9 *Bmp9*-KO pups injected with anti-BMP10 antibody presented a DA with a complete occlusion. This result was confirmed by angiography of the DA after injecting Evans blue in the ventricles. Indeed, whereas we could not detect any dye within the DA of *Bmp9*-KO pups, supporting that this DA is obstructed, we could see some blue dye in the center of the DA of *Bmp9*-KO pups treated with anti-BMP10 antibody, confirming that, in this case, the DA is open (Fig. 1*B*). Similar results were obtained with another anti-BMP10 neutralizing antibody developed in our laboratory (Fig. S1*A*). The specificity of these two neutralizing BMP10 antibodies versus other BMPs was also checked (Fig. S1*B*).

***Bmp9* Knockout Leads to Abnormal Closure of the DA at P4.** DA closure in mice has been shown to take place within a time frame of 1–3 h after birth (1). To understand what happened in these pups, we analyzed their DA at P0 (i.e., at least 8 h after birth), P3, and P4 through staining of semithin sections. In WT pups at P0, the center of the DA as delineated by the internal elastic lamina (IEL) was filled by cuboidal cells, which have previously been designated as intimal cells (ICs) because the nature of these cells is not clearly understood (1). These ICs were bordered by several layers of vascular smooth muscle cells (VSMCs) and elastic lamina (EL) (Fig. 2*A*). No difference could be detected at P0 between WT and *Bmp9*-KO pups, demonstrating that the absence of BMP9 did not affect the closure of the DA at this time point (Fig. 2*A*). At P3, WT, *Bmp9*-KO, and *Bmp9*-KO pups treated with an anti-BMP10 antibody still presented a closed DA (Fig. 2*B*). On the other hand, at P4, we observed major differences between these pups (Fig. 2*C*). Indeed, in contrast to WT pups, the center of the DA of *Bmp9*-KO pups was not completely

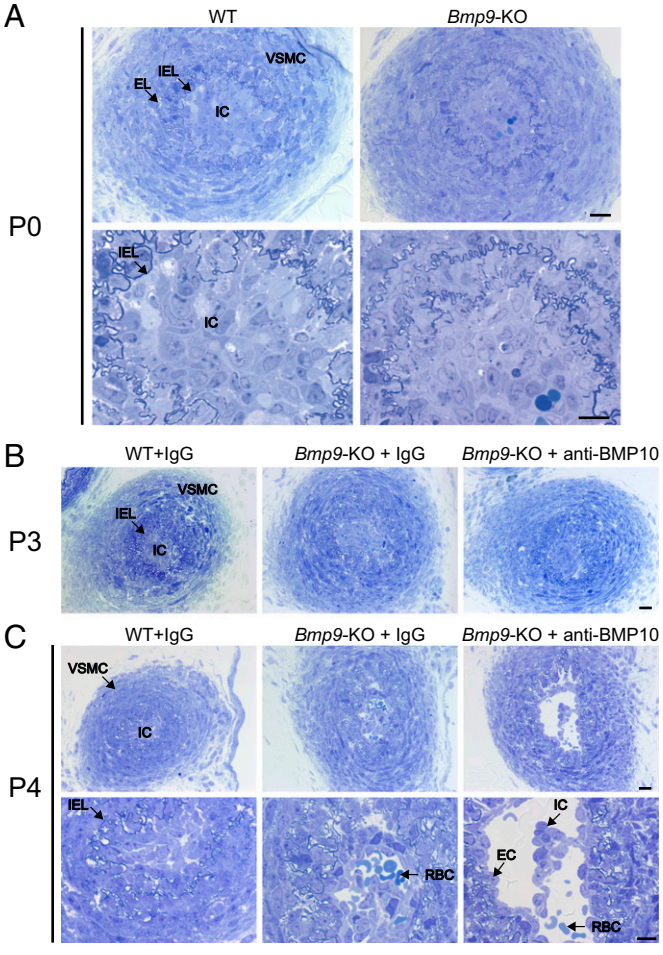


**Fig. 2.** Abnormal closure of the DA in *Bmp9*-KO pups at P4. Representative semithin transverse sections. (*A*) WT pups and *Bmp9*-KO pups were killed at P0. The DA center was filled with ICs, encircled by the IEL (the tortuous dark blue ribbon, seen at higher magnification) and surrounded by several layers of VSMCs and EL. (*B* and *C*) WT pups and *Bmp9*-KO pups were treated at P1 and P3 with IgG or an anti-BMP10 antibody and killed at P3 (*B*) or P4 (*C*). EC, endothelial cells; EL, elastic lamina; IC, intimal cells; IEL, internal elastic lamina; RBC, red blood cells; VSMC, vascular smooth muscle cells. [Scale bars: *A* and *C*, 20 μm (low magnification) and 10 μm (high magnification); *B*, 20 μm.]

filled with ICs, and red blood cells (RBCs) could be observed. This phenotype was exacerbated in *Bmp9*-KO pups treated with an anti-BMP10 antibody (Fig. 2*C*): the lumen was open, lined with a layer of flattened cells that looked like endothelial cells (ECs), and RBCs and islets of ICs could be detected in the lumen (Fig. 2*C*). Semithin cross-sections through the entire length of the DA and quantification of the remaining lumen area confirmed these results (Fig. S2). Taken together, these data demonstrate that injection of a neutralizing anti-BMP10 antibody to *Bmp9*-KO pups led to a reopening of the DA at P4. We could not determine whether this open DA eventually closes later on because *Bmp9*-KO pups treated with anti-BMP10 antibodies died between P4 and P6. We next asked whether the reopening process was time-dependent and thus treated *Bmp9*-KO pups with anti-BMP10 antibody at later times (P3 and P5). Interestingly, we did not observe a reopening of the DA at P6 or P7, demonstrating that BMP9 and BMP10 are critical during a short time window (between P1 and P3) for the proper remodeling of the DA into an irreversibly obstructed vessel.

***Bmp9* Knockout Leads to a Defect in DA Wall Thickening at Birth.** To better address the role of BMP9 in DA closure, we examined the first events associated with the closure. For this purpose, we performed a kinetic analysis of DA closure (0–5 h) in WT and *Bmp9*-KO pups immediately after caesarian section. As shown in Fig. 3*A*, the DA of both WT and *Bmp9*-KO pups was closed within 3 h after caesarian section. These data demonstrated that *Bmp9* inactivation did not affect functional closure of the DA.

Wall thickening is an important feature in the process of anatomical closure of the DA, which starts around birth in mice (1). We observed that DA wall thickness increased within the first hour after birth in WT pups whereas this increase was significantly reduced in *Bmp9*-KO pups (Fig. 3*B*). We next analyzed the DA of newborn pups at P0. Similarly, DA diameter was significantly reduced in *Bmp9*-KO pups versus WT pups (Fig. 3*C*). Hyaluronan (HA) production under the control of prostaglandins has been recently described to play a key role in DA closure (10). We therefore tested whether hyaluronan synthases (HAS) and cyclooxygenases (COX1 and -2), which were described as being the key enzymes for prostaglandin production in the DA (11), could be targets of BMP9 or BMP10 in endothelial cells [human pulmonary arterial endothelial cells (HPAECs)]. We found that BMP9 and BMP10 strongly increased *COX2* mRNA levels after 2 h stimulation whereas it did not affect *COX1* mRNA expression (Fig. 3*D*). HA is synthesized by three isoforms of HAS (HAS1, HAS2, and HAS3); we therefore studied mRNA expression of these three enzymes. Both *HAS2* and *HAS3* were detected in HPAECs whereas *HAS1* mRNA was not detectable. Interestingly, BMP9 and BMP10 were found to strongly increase *HAS2* mRNA levels after 4 h stimulation whereas it did not affect *HAS3* mRNA expression (Fig. 3*D*).

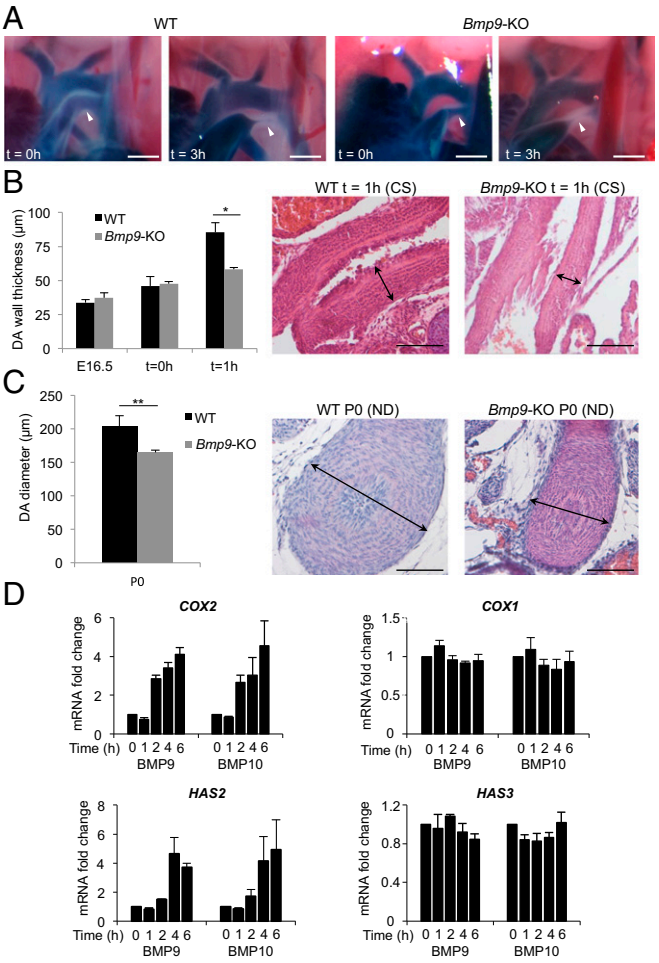


**Fig. 3.** Thickening defects in the DA of *Bmp9*-KO mice after birth. (*A*) Representative angiographic images of the DA (arrowhead) after Evans blue injection in the ventricles after caesarian section at term (E18.5, $t = 0$ h) and 3 h later ($t = 3$ h) in WT and *Bmp9*-KO pups. (WT, $n = 2$, $n = 2$, and *Bmp9*-KO, $n = 2$, $n = 2$, respectively from two littermates). (Scale bars: 500 µm.) (*B*) Quantification of the DA wall thickness in WT and B*mp9*-KO pups at E16.5, immediately after caesarian section (CS) at term (E18.5, $t = 0$ h) and 1 h later ($t = 1$ h) (WT, $n = 7$, $n = 4$, $n = 3$ and *Bmp9*-KO, $n = 5$, $n = 5$, $n = 3$, respectively) of H&E-stained longitudinal sections (representative images of 1 h after CS are shown). (Scale bars: 100 µm.) (*C*) Quantification of the DA diameter at P0 in WT and *Bmp9*-KO pups born by natural delivery (ND) ($n = 6$ in each group) of H&E-stained transverse sections of the DA (representative images are shown). (Scale bars: 100 µm.) $^{**}P \leq 0.01$ and $^{*}P \leq 0.05$ significantly different. (*D*) mRNA fold changes of *COX2*, *COX1*, *HAS2*, and *HAS3* expression in HPAECs stimulated with BMP9 or BMP10 (0.5 ng/mL). The results are represented as mRNA fold changes measured in BMP9- or BMP10-treated cells versus untreated cells at each time point. Data are the mean ± SEM from three independent experiments conducted in duplicate.

**BMP9 and BMP10 Are Necessary for Matrix Deposition During DA Remodeling.** To understand why the DA reopens in *Bmp9*-KO pups treated with anti-BMP10 antibodies, we analyzed transmission electron microscopy (TEM) images of the center of the DA at P0, P3, and P4. At P0, as previously described on semithin sections (Fig. 2*A*), the center of the DA was filled with compact cuboidal, referred to as ICs, and no difference could be detected between WT and *Bmp9*-KO pups (Fig. 4*A*). These cells were in both cases highly synthetic, containing abundant rough endoplasmic reticulum, and tiny desmosome-like junctions (DLJs) were occasionally observed between cells (see *Insets* in Fig. 4*A*). At P3, in WT pups, numerous ICs were surrounded by matrix deposition (MD) (Fig. 4*B*), which could not be detected at P0 (Fig. 4*A*). Interestingly, in contrast to WT pups, we could not detect MD between ICs at P3 in *Bmp9*-KO pups treated with an anti-BMP10 antibody whereas DLJ could still be observed (Fig. 4*B*). *Bmp9*-KO pups, at P3, gave an intermediary phenotype with areas of ICs with MD and areas without. At P4, in WT pups, nearly all of the cells within the DA center were surrounded with MD (Fig. 4*C*). In contrast, at P4, the DA of *Bmp9*-KO pups treated with an anti-BMP10 antibody was open, and, interestingly, this lumen was lined with a layer of flattened endothelial cells (ECs), tightly connected, polarized toward the lumen and containing Weibel–Palade bodies (WPBs) (Fig. 4*C*). Similar features, although not as pronounced, were observed in *Bmp9*-KO pups treated with IgG (Fig. 4*C*). Several extracellular matrix (ECM) proteins have been described to be involved in DA closure, among which is fibronectin (12). Because we observed defect in matrix deposition in *Bmp9*-KO mice, we tested whether

BMP9 and BMP10 could regulate the protein expression of fibronectin and also type I collagen. We found that BMP9 and BMP10 strongly induced the expression of fibronectin in endothelial cells whereas they did not affect the expression of type I collagen (Fig. 4*D*). Quantitative RT-PCR of isolated DA demonstrated the presence of the receptors ALK1, BMPR2, and ActR2A and the coreceptor endoglin, supporting that cells from the DA can respond to the BMP9/BMP10 signaling pathway (Table S1). Accordingly, 48-h BMP9 treatment of ex vivo cultures of great arteries (i.e., DA, PA, and aortic arch) induced the expression of the specific transcription factor inhibitor of differentiation 1 (Id1) and fibronectin (Fig. 4*E*).

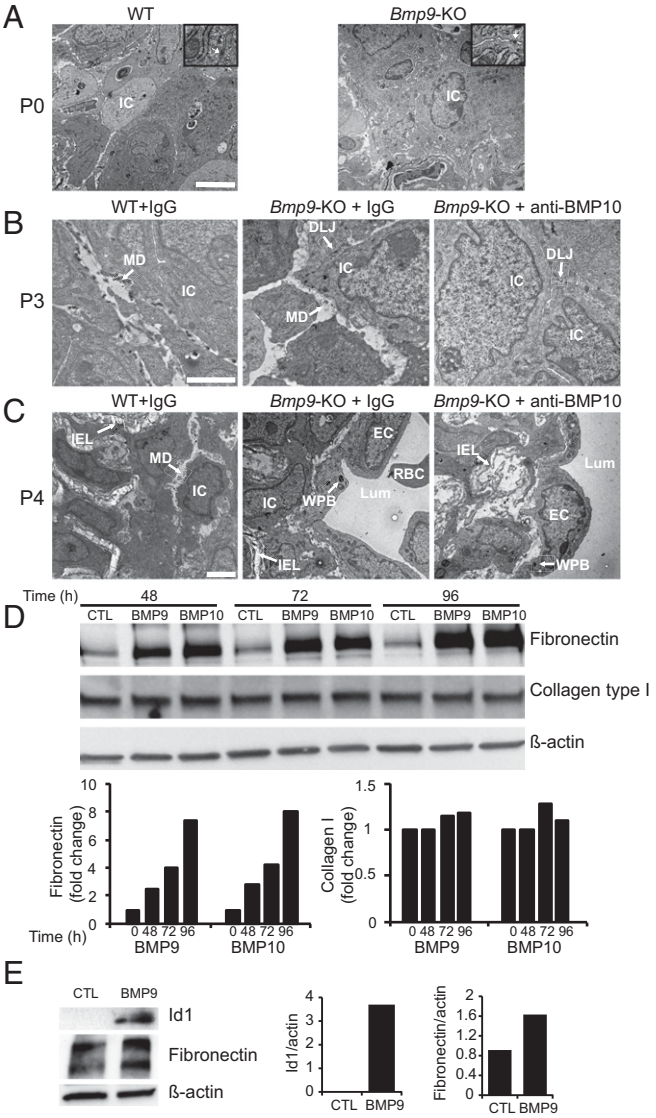


**Fig. 4.** BMP9 and BMP10 are necessary for matrix deposition during DA remodeling. (*A*–*C*) Transmission electron microscopy (TEM) images of the DA center. (*A*) At P0 in WT and *Bmp9*-KO pups. (Scale bar: 5 μm.) (*Insets*) Sevenfold higher magnifications (white arrows show desmosome-like junctions (DLJs). (*B*) At P3 in WT pups and *Bmp9*-KO pups treated at P1 with IgG or an anti-BMP10 antibody. (Scale bar: 2 μm.) (*C*) At P4 in WT pups and *Bmp9*-KO pups treated at P1 and P3 with IgG or an anti-BMP10 antibody. (Scale bar: 2 μm.) DLJ, desmosome-like junctions; EC, endothelial cells; IC, intimal cells; IEL, internal elastic lamina; Lum, Lumen; MD, matrix deposition; RBC, red blood cells; WPB, Weibel–Palade bodies. (*D*) HPAECs were incubated with or without BMP9 or BMP10 (10 ng/mL) for the indicated times. (*E*) WT great arteries (pool of three pups), dissected at P1, were stimulated with or without BMP9 (10 ng/mL) for 48 h. (*D* and *E*) Cell lysates (20- and 10-μg proteins, respectively) were resolved by SDS/PAGE and immunoblotted with antibodies against fibronectin, collagen type I, Id1, and β-actin. Quantifications of the Western blots normalized to β-actin are shown (one representative experiment out of four and two, respectively).

**BMP9 and BMP10 Are Involved in the Process of DA Anatomical Closure.** We next addressed what was the origin of the ICs that filled the center of the DA at P0. For this purpose, we performed double immunofluorescence staining for CD31, also known as PECAM, an endothelial specific marker and fibronectin. We found that, at P0, the majority of ICs were CD31-positive, supporting that ICs are endothelial cells (ECs) (Fig. 5*A*). Analysis of the center of the DA between P0 and P5 clearly demonstrated that the number of $CD31^+$ cells significantly decreased with time. Inversely, fibronectin staining within the DA center increased from P0 to P5, supporting that fibronectin is one of the protein of the MD (Fig. 5*A*). We next searched for the mechanism responsible for the loss of ECs in the DA center. Apoptotic ECs, identified via active caspase 3 staining, and dense fragmented nuclei (white arrows) could already be detected at P0 (Fig. 5*B*, *Left*). Apoptosis was further supported by TEM images; picnotic nuclei (white asterisk) and apoptotic bodies (black arrow) could be identified (Fig. 5*B*, *Middle*). We also observed, on TEM images, large double-membrane vesicles that resembled autophagosomes (white asterisk, Fig. 5*B*, *Right*). Thus, EC loss could be at least partially due to cell death.

The center of the DA can be delineated by elastin staining, which decorates all elastic lamina, including the IEL. Interestingly, costaining of the DA at P5 with an antibody directed against elastin, and CD31 or the mesenchymal marker α smooth muscle actin (α-SMA), revealed that, within the DA center, the remaining CD31 cells were surrounded by α-SMA–positive cells (Fig. 5*C*, *Left*). This result suggested that some ECs had acquired a mesenchymal phenotype. Indeed, we detected as soon as P0 some cells that expressed both CD31 and α-SMA (white arrowhead) reflecting early endothelial-to-mesenchymal transition (endMT) (Fig. 5*C*, *Middle*). This result was further supported by TEM image: Fig. 5*C*, *Right* shows a polarized EC cell (cell 1) facing the lumen still connected (white arrowhead) to another cell (cell 2) acquiring a mesenchymal phenotype surrounded by MD (asterisks).

Interestingly, the number of CD31-positive cells at P3 in *Bmp9*-KO pups injected with anti-BMP10 antibodies was significantly higher than in WT pups, suggesting an impairment in the decrease of ECs under these conditions (Fig. 5*D*). This result was further supported by measuring the expressions of CD31 and p120-catenin, a cytoplasmic scaffold protein binding to VE-cadherin that determines the stability of adheren junctions (13), which were higher in *Bmp9*-KO pups injected with anti-BMP10 antibodies versus WT pups (Fig. 5*E*). Taken together, these results support that BMP9 and BMP10 could take part in a process of endMT occurring during DA vascular remodeling.

**BMP9 and BMP10 Up-Regulate the Expression of Transcription Factors Involved in endMT.** To further support this hypothesis and to extend our findings beyond the KO mouse, we analyzed the effect of BMP9 and BMP10 in HPAECs on the expression of transcription factors known to be involved in the process of epithelial-to-mesenchymal transition (EMT) and endMT (14). We found that BMP9 and BMP10 very rapidly (within 1 h) and transiently up-regulated (between four- and sevenfold) the expression of *SNAI1* and *SNAI2* (Fig. 6 *A* and *B*). Interestingly, BMP9 and BMP10 also up-regulated the expression of *ZEB2, TWIST1*, and *FOXC2,* although in a delayed manner in comparison with *SNAI1* and *SNAI2*, without affecting the expression of *ZEB1* (Fig. 6 *C*–*F*).

**Identification of a Deleted Minimal Critical Region Linked with Patent Ductus Arteriosus in Humans.** Several genes and chromosomal deletions have been associated with PDA (4, 15). We therefore

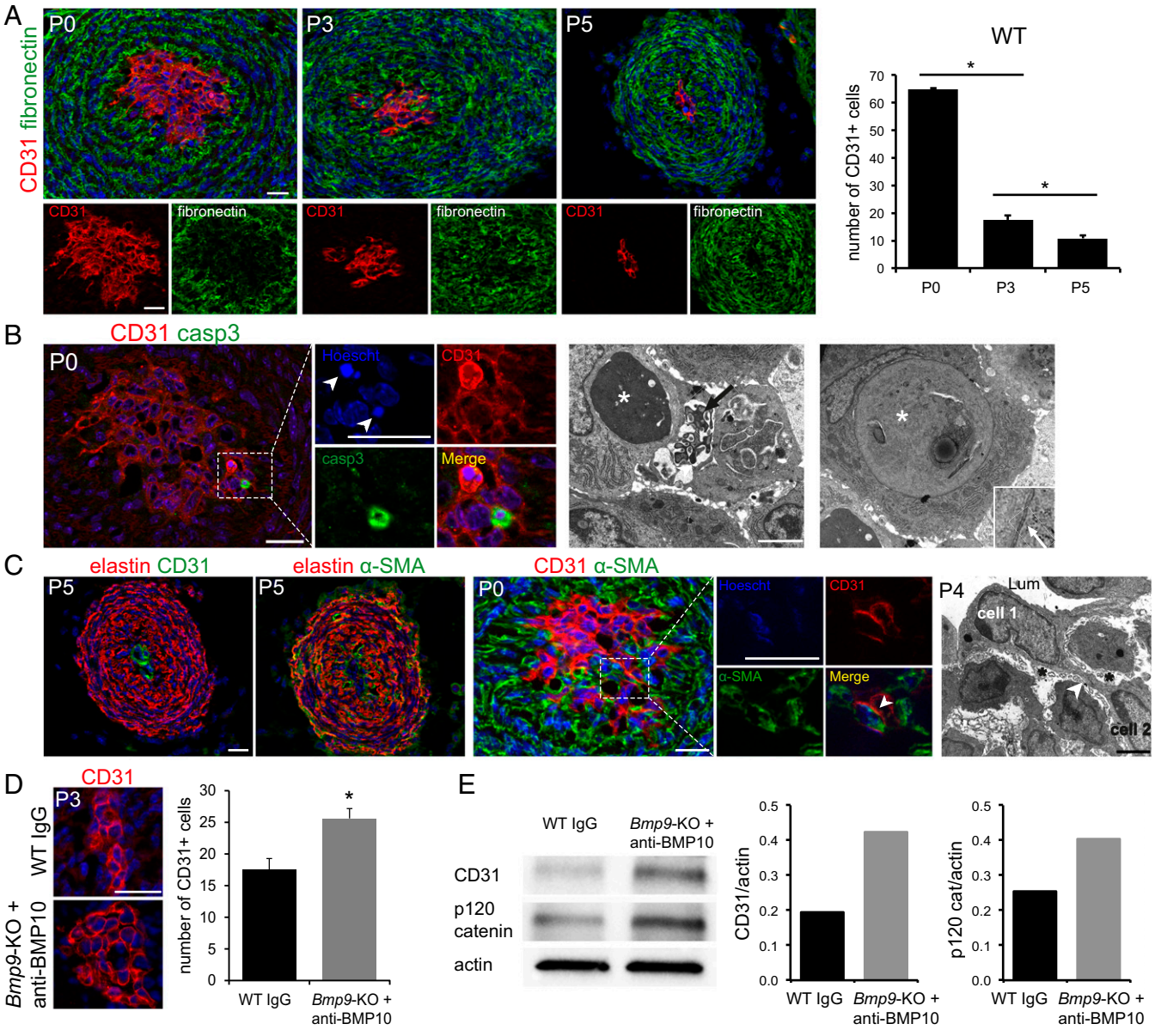


**Fig. 5.** BMP9 and BMP10 are involved in the process of DA anatomical closure. (*A*) Representative immunofluorescence staining of CD31 and fibronectin of a WT DA at P0, P3, and P5 and higher magnifications. The graph bar indicates the number of CD31$^+$ cells (P0 $n = 3$ from two littermates, P3 $n = 6$ from four littermates, and P5 $n = 3$ from two littermates), data are the mean ± SEM. (*B*) Active caspase-3 staining (*Left*) and higher magnifications, and TEM images. (*Middle*) Picnotic nuclei (white asterisk) and apoptotic bodies (black arrow). (*Right*) Double-membrane vesicle that could correspond to an autophagosome (white asterisk). (*Inset*) A higher magnification (white arrow shows the double-membrane). (*C*) Double immunofluorescence staining of elastin and CD31, elastin and α-SMA, and CD31 and α-SMA, and higher magnifications (white arrowhead pointing a double CD31 and α-SMA–positive cell), and TEM image of the DA center (*Right*) showing a cell (cell 1) polarized facing the lumen (Lum) connected (arrow) to another cell (cell 2) acquiring a mesenchymal phenotype surrounded by matrix (black asterisks). (*D*) Representative immunofluorescence staining of CD31 at P3 of a WT DA and a *Bmp9*-KO pup treated with anti-BMP10 antibodies at P1. The graph bar indicates the number of CD31$^+$ cells ($n = 6$ from four littermates and $n = 5$ from two littermates, respectively; data are the mean ± SEM). (*E*) Ten micrograms of cell lysates obtained at P3 from WT and *Bmp9*-KO DA injected with anti-BMP10 antibodies at P1 (n = 6 for each sample from three littermates) were resolved by SDS/PAGE and immunoblotted with antibodies against CD31, p120-catenin, and β-actin. Quantifications of the Western blots normalized to β-actin are shown (one representative experiment out of two). (Scale bars: IF, 20 μm and TEM, 5 μm.) *$P \leq 0.05$ significantly different.

looked whether patients with PDA would present a chromosomal deletion of *BMP9* or *BMP10*. The information gathered in the database of genomic variants (DGV) showed the presence of many polymorphic copy number variations (CNVs) in the *BMP9* gene. These data suggest that haploinsufficiency of the *BMP9* gene is not directly involved in a specific disease. In contrast, no polymorphic CNVs including *BMP10* were found. Moreover, we identified two patients with a syndromic PDA that had a large heterozygous deletion including the entire *BMP10* gene, each presenting a PDA among other clinical features (Fig. 7). In patient 1, array-comparative genomic hybridization (CGH) analysis showed a 4.62-Mb deletion in chromosome band 2p14-p13.3 extending from base pair 65,561,711 to 70,187,280 [National Center for Biotechnology Information (NCBI); hg 19] from the 2p telomere (Fig. 7). This 4.62-Mb heterozygous deletion arose de novo because it could not be found in the parental analysis and contained more than 28 known protein-coding genes. Patient 2 also harbored a de novo 7-Mb deletion in chromosome

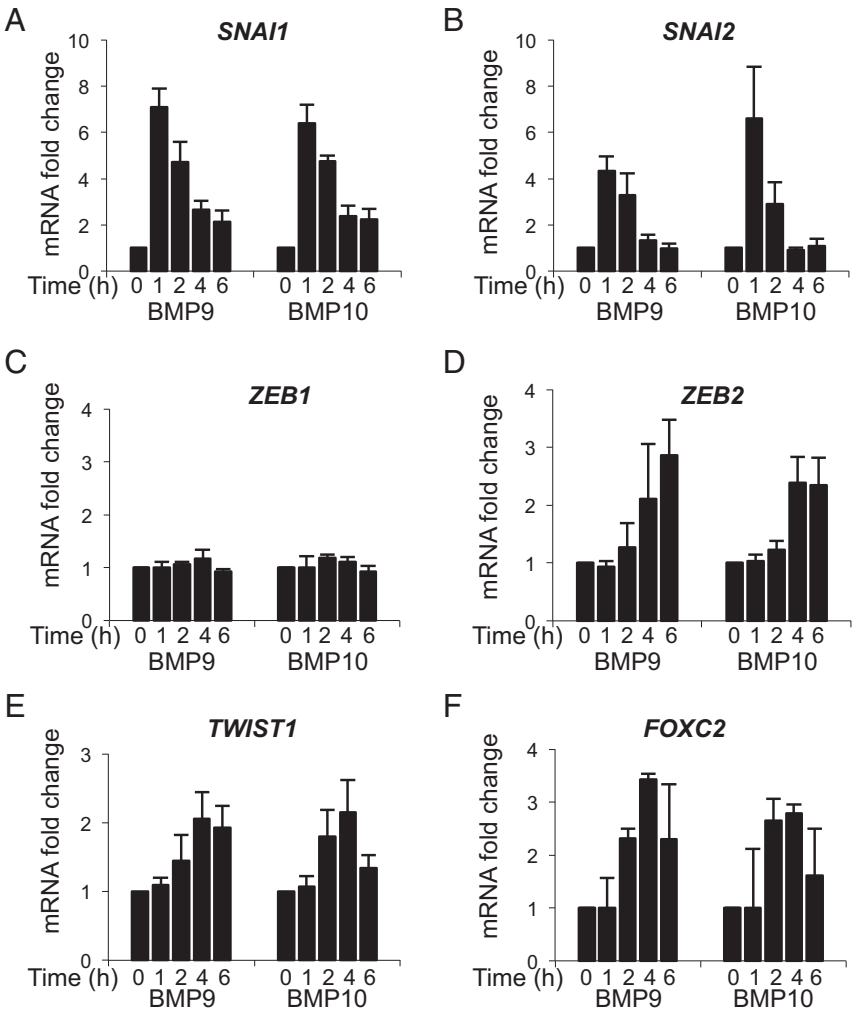


**Fig. 6.** BMP9 and BMP10 regulate several transcription factors known to be involved in epithelial-to-mesenchymal transition. (*A–F*) HPAECs were stimulated with BMP9 or BMP10 (0.5 ng/mL) for the indicated times. Expression of HPRT was used to normalize the samples. The results are represented as mRNA fold changes measured in BMP9- or BMP-10 treated cells versus nontreated cells at each time point. Data are the mean ± SEM from three independent experiments performed in duplicates.

bands 2p15-p13.3, including about 75 known protein-coding genes. This deletion extended from base pair 63,921,609 to 70,915,279 from the 2p telomere (NCBI; hg 19) (Fig. 7). Six other patients, with several deletions overlapping these two anomalies, but excluding *BMP10*, did not show any cardiac abnormality (no PDA). By collecting all these data, we were able to define a 700-kb minimal critical region (MCR) that correlated with the presence of a PDA. This MCR included *BMP10* among seven other genes (*APLF, PLEK, FBX048, GKN2, PROKR1, CNRIP1, ARHGAP25*). Although preliminary, these results of human genetics provided an additional argument for the involvement of at least BMP10 in the physiopathology of the PDA.

## Discussion

This study shows, for the first time, to our knowledge, a critical role for BMP9 and BMP10 in the closure of the DA. This process has been described to occur following two phases, the functional and the anatomical (3). Our data demonstrate that BMP9 is not necessary for the functional closure of the DA. On the other hand, the data reveal that BMP9 is important for proper anatomical closure to occur and that BMP9 can be partially replaced by BMP10. However, if we add an anti-BMP10 antibody to *Bmp9*-KO pups during a specific time window (between P1 and P3), then the anatomical closure process fails and the DA reopens.

Anatomical closure of the DA starts with intimal thickening of the DA. This process is initiated prenatally or at birth, depending on the size of the animal, with the development of intimal cushions, and is completed postnatally by humoral and mechanical stimuli (3, 4). $PGE_2$ elicits the deposition of HA within the intimal tissue and stimulates the inward migration of VSMCs (10). The present data further support that wall thickening, in mice, starts within the first hour after birth (1). Interestingly, we found that this process is significantly reduced in *Bmp9*-KO, demonstrating that BMP9 is necessary for this step and that it cannot be compensated by BMP10. Several glycoproteins and glycosaminoglycans are involved in wall thickening of the DA. Especially, HA is produced by both ECs and VSMCs, and its deposition creates a hygroscopic environment suitable for cell migration (16, 17). In accordance with a previous study in human umbilical vein endothelial cells (HUVECs) (18), only *HAS2* and *HAS3* mRNA were detected in HPAECs. We showed that BMP9 and BMP10 specifically regulated *HAS2* mRNA expression. This result further supported the work reported by Yokoyama et al., who found that, among the three HAS isoforms, HAS2 was largely responsible for HA production in the DA (10). $PGE_2$ is the principal activator of HA production in the DA, and COX2 has been described as the most important COX in the closure of the DA (11). Interestingly, we found that *COX2* mRNA expression, but not *COX1*, was strongly induced by BMP9 and

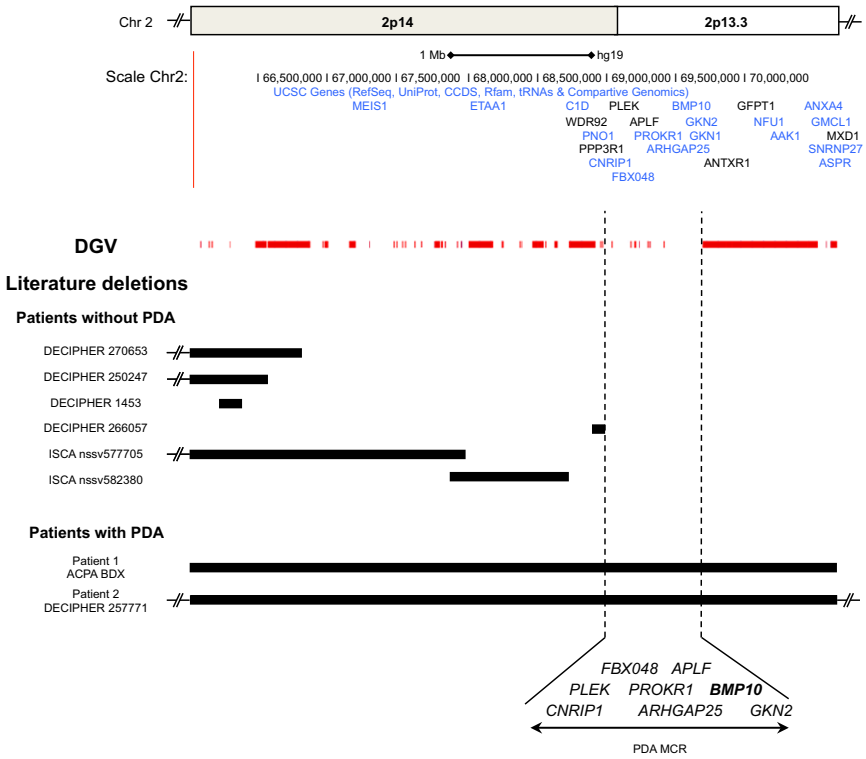


**Fig. 7.** Identification of a deleted minimal critical region of 700 kb associated with patent ductus arteriosus (PDA) in humans. Schematic representation of the human chromosome region 2p13.3–2p14 using the University of California, Santa Cruz (UCSC) genome browser (genome.ucsc.edu/). (*Upper*) Ideogram of the chromosome region 2p13.3–2p14 with the physical positions of the genes. (*Lower*) All genomic deletions in this region reported in the literature and in our patients are represented with solid black bars. Well-known benign deletions reported in the DGV (Database of Genomic Variants) are represented with solid red bars. The 700-kb minimal critical region (MCR) correlated with the presence of a PDA is highlighted by dashed lines. The candidate genes included in this MCR are highlighted. Interestingly, among them was identified *BMP10* (bold).

BMP10. These data thus suggest that BMP9 and BMP10 are important regulators of HAS2 and COX2 expression and that downregulation of their expression could in part result in the defect in wall thickening observed in *Bmp9*-KO pups.

We show in the present work that, at P0, the DA center, as delineated by the IEL, is filled by endothelial cells (ECs) (Fig. 5), in accordance with the work of Echtler et al. (19). Thus, the intimate cells that obstruct the DA are mostly of endothelial origin. Analyses of TEM images of WT pups showed, at P0, that ECs were arranged densely and compactly. However, at P3, these cells became gradually dissociated from one another and were surrounded by matrix deposition. Fibronectin has been shown to be critical in DA closure and in particular for smooth muscle migration into the subendothelium and intimal cushion formation (12). Our data support that fibronectin is one of the matrix proteins surrounding these intimal cells. Importantly, we show that the number of ECs strongly decreased between P0 and P5. This loss of endothelial cells together with an increase in matrix deposition recalls the process of endMT. This hypothesis is supported by TEM images but also by the coexpression of endothelial and mesenchymal markers within few cells. Still, the loss of ECs from P0 to P5 might not only be due to endMT because apoptosis, as shown by active caspase 3 staining and TEM images, could be observed in the DA in agreement with previous works (20, 21). We also observed on TEM images double-membrane vesicles that resemble autophagosomes and therefore suggest that autophagy could also occur in DA remodeling. Taken together, these data would propose that anatomical remodeling of the DA involves endMT and apoptosis, as depicted in the working model in Fig. 8*A*.

The involvement of the TGFβ family has been previously described in DA remodeling (12, 22, 23). The present work further supports that this signaling family could play a major role in this process. We show here that injection of anti-BMP10 antibodies to *Bmp9*-KO pups during a very short time window (P1 to P3) leads to a reopening of the DA at P4. Analysis of these DA at P3 showed a defect of MD and a higher number of ECs correlated to an increase in the expression of CD31 and p120-catenin proteins. In parallel, we found that BMP9 and BMP10 induced the expression of fibronectin in isolated HPAECs but also in isolated DA. We also found that BMP9 and BMP10 strongly induced the mRNA expression of several transcription factors (*SNAI1, SNAI2, ZEB2, TWIST1*, and *FOXC2*) known to be important in the initiation of EMT or endMT (14). In accordance, it has already been described that BMP9 and BMP10 transiently induce the expression of *HEY1, HEY2*, and *HES1* (8, 24), which are transcription factors of the Notch signaling pathway also known to be involved in EMT (14). Taken together, these data allow us to propose that, in *Bmp9*-KO pups injected with anti-BMP10 antibody (P1 and P3), ECs fail to go through a transition into a mesenchymal-like phenotype, and this defect of remodeling leads to loose cell interactions that will result in the reopening of the DA. This working model, which calls for further work to be validated, is presented in Fig. 8*B*. Our data further support the involvement of the BMP signaling pathway in endMT. Indeed, although TGFβ is one of the most potent inducers of EMT (14), the role of BMPs is still not completely clear (25). BMPs have been described as either inhibitors of endMT (BMP7 in cardiac fibrosis) (26) or inducers of endMT [BMP6 in cerebral cavernous malformations (27) and BMP2 in cardiac valve formation (28)]. BMP9 has been recently shown to induce EMT in hepatocellular carcinoma cells (29), and our data support that BMP9 and BMP10 can also induce endMT.

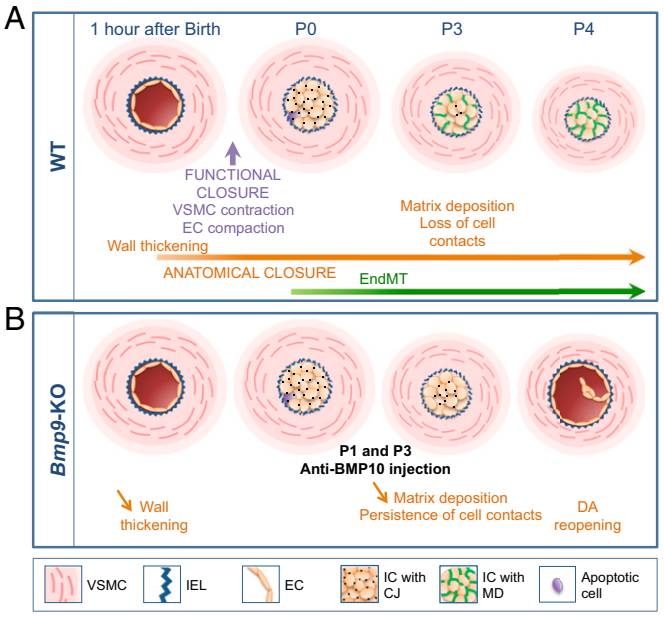


**Fig. 8.** A schematic working model of DA closure in WT and *Bmp9*-KO pups treated with anti-BMP10 antibodies. (*A*) In WT pups, functional closure occurs within 3 h after birth due to VSMC contraction and EC compaction. Anatomical closure encompasses wall thickening that starts within the first hour after birth and vascular remodeling, which takes several days. At P0, the DA center is filled by cuboidal intimal cells (ICs) that we show here to be endothelial cells (ECs). These ECs are connected to each other by cell junctions (CJs). These ECs will rapidly lose their intercellular contacts (P3) and increase their matrix deposition (MD): We propose that this process involves endothelial-to-mesenchymal transition (endMT). A few apoptotic cells within the center of the DA could also be found. (*B*) In *Bmp9*-KO pups, functional closure normally occurs. The first steps of anatomical closure, corresponding to wall thickening and vascular remodeling, are partially affected. Injection of anti-BMP10 antibodies to these pups seems to exacerbate this imperfect vascular remodeling, resulting in the persistence of cell contacts with CJs, the absence of MD between ICs at P3, and the maintenance of CD31-positive cells. We propose that the observed defect in anatomical closure occurs through endMT inhibition. In the absence of endMT, subjected to the pressure of blood flow, these ECs will return to a flattened phenotype and will ultimately lead to the reopening of the DA at P4.

PDA in human infants can be divided into two groups: a common condition present in very preterm infants that would not be present if these infants had been born at term and a relatively rare condition seen in term infants that is associated with genetic abnormalities. In this case, PDA exists as part of a constellation of other physical anomalies. Online Mendelian Inheritance in Man (www.ncbi.nlm.nih.gov/omim) lists more than 100 disorders in which PDA is found, supporting the idea that single genes can contribute to syndromic PDA (15). The presence of a PDA with only minor cardiac defects has been particularly well-characterized with mutations in three genes (*MYH11, ACTA2, TFAP2B*) (15). In the present study, genetic analysis in national and international databases allowed us to define a 700-kb minimal critical region (MCR) including *BMP10* along with only seven other genes (*APLF, PLEK, FBX048, GKN2, PROKR1, CNRIP1, ARHGAP25*). These results provided an additional argument for the involvement of BMP10 in the physiopathology of PDA. However, these encouraging results require confirmation and further molecular analyses of the *BMP10* gene in a larger cohort of patients with isolated PDA. It is interesting to note that mutations in the TGFβ signaling pathway have been previously associated with PDA, such as in Loeys–Dietz syndrome (4).

Our research emphasizes the role of the TGFβ family and more particularly of BMP9 and BMP10 in vascular development and postnatal vascular remodeling. In addition to their roles in lymphatic development, cardiac development, and postnatal retinal vascularization (8, 30, 31), we now show that BMP9 and BMP10 are also important for the closure of the DA. This result is in accordance with the high circulating levels of BMP9 and BMP10 in mice around birth (7, 8). It will be interesting in the future to measure circulating levels of BMP9 and BMP10 in term and preterm infants to test whether there is also an increase in these two factors around birth, and whether we can correlate the circulating levels of these BMPs with the risk of PDA.

Research on PDA has already provided clinical applications. Nevertheless, management of premature infants with PDA remains troublesome and calls for alternative approaches to the prostaglandin $E_2$ inhibitors now in use (32). The involvement of BMP9 and BMP10 in the anatomical closure of the DA process is an important finding with potential clinical applications in the management of this pathology.

## Materials and Methods

**Mice.** All animal studies were approved by the institutional guidelines and those formulated by the European Community for the Use of Experimental Animals. Heterozygous offspring of chimeras were mated out of nine generations to C57BL6/J as previously described (8). Anti-BMP10 (15 mg/kg, MAB2926; R&D Systems; or clone 13C11; from our laboratory) monoclonal antibodies or control IgG were injected intraperitoneally (i.p.) in mice at P1 and P3. Pups were killed at P0, P3, P4, or P5. Preterm and term fetuses were delivered by cesarean section at 16.5 and 18.5 d postcoitum, respectively. For the later, corresponding to a few hours before natural delivery, pups were killed every hour (until 5 h) for histological analysis.

**Microscopy.** For light microscopy and immunofluorescence, embryos from embryonic day 16.5 (E16.5) and E18.5 obtained after Caesarean section and pups from P0 and P5 were fixed in 4% (wt/vol) paraformaldehyde overnight at 4 °C and embedded in OCT for frozen sections or in paraffin. Frozen sections were stained using antibodies to fibronectin (AB2033; Millipore), CD31 (clone MEC13; BD), α-SMA (A5228; Sigma), elastin (PR385, tropoelastin; Elastin Products), and active caspase-3 (AF835; R&D Systems) and paraffin sections using antibodies to CD31 (53332, Anaspec; Eurogentec). For transmission electron microscopy, chest cavities of P0, P3, and P4 mice were filled with 2.5% (wt/vol) glutaraldehyde in 0.1 M sodium cacodylate (pH 7.2), and DA were then dissected and fixed overnight at 4 °C. Semithin (0.5-μm) and thin (90-nm) sections were observed by light and electron microscopy, respectively. For further details, see *SI Materials and Methods*.

**Endothelial Cell Culture, Treatment, Quantitative Real-Time PCR, and Western Blot Analysis.** Human pulmonary arterial endothelial cells (HPAECs) were stimulated with recombinant human BMP9 or BMP10 (R&D Systems), and Real-Time PCR (RT-PCR) and Western blot analyses were performed as indicated in *SI Materials and Methods*.

**Protein Extraction from DA.** To study the ex vivo effect of BMP9 on the DA, great arteries (including the DA and the aortic arch arteries) were dissected from WT pups at P1 after killing by decapitation. Great arteries were cultured for 48 h in DMEM with or without BMP9 (10 ng/mL), and then lysed in radioimmunoprecipitation assay (RIPA) buffer. At least three great arteries were pooled for each condition.

To study the in vivo effect of anti-BMP10 injection at P1 in *Bmp9*-KO pups versus WT pups treated with IgG, isolated DA were dissected at P3 from killed pups after decapitation. At least six DA were pooled for each condition.

In both cases, proteins were extracted using Precellys lysing tubes and analyzed by Western blot as indicated in *SI Materials and Methods*.

**Human Genomic Analysis.** All samples were obtained from subjects after an institutional review board approved informed consent (DGS 2004/0341). The study protocol was approved by the Grenoble institutional review board (IRB no. 6705). A search for individuals carrying CNVs encompassing *BMP9* or *BMP10* genes was made in French (AchroPuce) and international databases [Database of Chromosomal Imbalance and Phenotype in Humans using Ensembl Resources (DECIPHER) and (International Standards for Cytogenomic Arrays Consortium (ISCA)] of patients and healthy controls (DGV) analyzed by array-CGH. For further details, see *SI Materials and Methods*.

**Statistical Analysis.** Statistical data analysis was assessed using the Mann–Whitney test or Fisher's exact test, as indicated.

**ACKNOWLEDGMENTS.** We thank the animal unit staff at Institut de Recherches en Technologies et Sciences pour le Vivant (iRTSV) for animal husbandry, Dr. S. J. Lee (Johns Hopkins University School of Medicine) and Dr. T. Zimmers (Thomas Jefferson University) for providing the *Bmp9*$^{-/-}$ mice, and Dr. O. Filhol and M. Prioux for sharing some PCR primers. This work was supported by INSERM (U1036), CEA, Université Joseph Fourier (UJF), Association pour la Recherche sur le Cancer Grant SFI20111203720, the Groupement d'Entreprises Françaises de Lutte Contre le Cancer (GEFLUC) Dauphiné-Savoie, the Ligue Contre le Cancer de la Loire et de la Savoie, Association Maladie de Rendu-Osler (AMRO), and a Fondation Lefoulon-Delalande postdoctoral grant (to D.C.).

1. Tada T, Kishimoto H (1990) Ultrastructural and histological studies on closure of the mouse ductus arteriosus. *Acta Anat (Basel)* 139(4):326–334.
2. Bergwerff M, DeRuiter MC, Gittenberger-de Groot AC (1999) Comparative anatomy and ontogeny of the ductus arteriosus, a vascular outsider. *Anat Embryol (Berl)* 200(6):559–571.
3. Coceani F, Baragatti B (2012) Mechanisms for ductus arteriosus closure. *Semin Perinatol* 36(2):92–97.
4. Bökenkamp R, DeRuiter MC, van Munsteren C, Gittenberger-de Groot AC (2010) Insights into the pathogenesis and genetic background of patency of the ductus arteriosus. *Neonatology* 98(1):6–17.
5. Bailly S (2014) BMP9, BMP10 and ALK1: An emerging vascular signaling pathway with therapeutic applications. *Molecular Mechanisms of Angiogenesis: From Ontogenesis to Oncogenesis*, eds Feige JJ, Pagès G, Soncin F (Springer, Paris), pp 99–119.
6. David L, Mallet C, Mazerbourg S, Feige JJ, Bailly S (2007) Identification of BMP9 and BMP10 as functional activators of the orphan activin receptor-like kinase 1 (ALK1) in endothelial cells. *Blood* 109(5):1953–1961.
7. Bidart M, et al. (2012) BMP9 is produced by hepatocytes and circulates mainly in an active mature form complexed to its prodomain. *Cell Mol Life Sci* 69(2):313–324.
8. Ricard N, et al. (2012) BMP9 and BMP10 are critical for postnatal retinal vascular remodeling. *Blood* 119(25):6162–6171.
9. Chen H, et al. (2004) BMP10 is essential for maintaining cardiac growth during murine cardiogenesis. *Development* 131(9):2219–2231.
10. Yokoyama U, et al. (2006) Chronic activation of the prostaglandin receptor EP4 promotes hyaluronan-mediated neointimal formation in the ductus arteriosus. *J Clin Invest* 116(11):3026–3034.
11. Loftin CD, et al. (2001) Failure of ductus arteriosus closure and remodeling in neonatal mice deficient in cyclooxygenase-1 and cyclooxygenase-2. *Proc Natl Acad Sci USA* 98(3):1059–1064.
12. Rabinovitch M (1996) Cell-extracellular matrix interactions in the ductus arteriosus and perinatal pulmonary circulation. *Semin Perinatol* 20(6):531–541.
13. Ranchoux B, et al. (2015) Endothelial-to-mesenchymal transition in pulmonary hypertension. *Circulation* 131(11):1006–1018.
14. Lamouille S, Xu J, Derynck R (2014) Molecular mechanisms of epithelial-mesenchymal transition. *Nat Rev Mol Cell Biol* 15(3):178–196.
15. Hajj H, Dagle JM (2012) Genetics of patent ductus arteriosus susceptibility and treatment. *Semin Perinatol* 36(2):98–104.
16. De Reeder EG, et al. (1988) Hyaluronic acid accumulation and endothelial cell detachment in intimal thickening of the vessel wall: The normal and genetically defective ductus arteriosus. *Am J Pathol* 132(3):574–585.
17. Boudreau N, Turley E, Rabinovitch M (1991) Fibronectin, hyaluronan, and a hyaluronan binding protein contribute to increased ductus arteriosus smooth muscle cell migration. *Dev Biol* 143(2):235–247.
18. Vigetti D, et al. (2010) Proinflammatory cytokines induce hyaluronan synthesis and monocyte adhesion in human endothelial cells through hyaluronan synthase 2 (HAS2) and the nuclear factor-kappaB (NF-kappaB) pathway. *J Biol Chem* 285(32):24639–24645.
19. Echtler K, et al. (2010) Platelets contribute to postnatal occlusion of the ductus arteriosus. *Nat Med* 16(1):75–82.
20. Tananari Y, et al. (2000) Role of apoptosis in the closure of neonatal ductus arteriosus. *Jpn Circ J* 64(9):684–688.
21. Imamura S, Nishikawa T, Hiratsuka E, Takao A, Matsuoka R (2000) Behavior of smooth muscle cells during arterial ductal closure at birth. *J Histochem Cytochem* 48(1):35–44.
22. Boudreau N, Clausell N, Boyle J, Rabinovitch M (1992) Transforming growth factor-beta regulates increased ductus arteriosus endothelial glycosaminoglycan synthesis and a post-transcriptional mechanism controls increased smooth muscle fibronectin, features associated with intimal proliferation. *Lab Invest* 67(3):350–359.
23. Tannenbaum JE, et al. (1995) Transforming growth factor beta 1 inhibits fetal lamb ductus arteriosus smooth muscle cell migration. *Pediatr Res* 37(5):561–570.
24. Larrivée B, et al. (2012) ALK1 signaling inhibits angiogenesis by cooperating with the Notch pathway. *Dev Cell* 22(3):489–500.
25. Medici D, Kalluri R (2012) Endothelial-mesenchymal transition and its contribution to the emergence of stem cell phenotype. *Semin Cancer Biol* 22(5-6):379–384.
26. Zeisberg EM, et al. (2007) Endothelial-to-mesenchymal transition contributes to cardiac fibrosis. *Nat Med* 13(8):952–961.
27. Maddaluno L, et al. (2013) EndMT contributes to the onset and progression of cerebral cavernous malformations. *Nature* 498(7455):492–496.
28. Luna-Zurita L, et al. (2010) Integration of a Notch-dependent mesenchymal gene program and Bmp2-driven cell invasiveness regulates murine cardiac valve formation. *J Clin Invest* 120(10):3493–3507.
29. Li Q, et al. (2013) Bone morphogenetic protein-9 induces epithelial to mesenchymal transition in hepatocellular carcinoma cells. *Cancer Sci* 104(3):398–408.
30. Levet S, et al. (2013) Bone morphogenetic protein 9 (BMP9) controls lymphatic vessel maturation and valve formation. *Blood* 122(4):598–607.
31. Chen H, et al. (2013) Context-dependent signaling defines roles of BMP9 and BMP10 in embryonic and postnatal development. *Proc Natl Acad Sci USA* 110(29):11887–11892.
32. Hamrick SE, Hansmann G (2010) Patent ductus arteriosus of the preterm infant. *Pediatrics* 125(5):1020–1030.